Biointerphases
A Journal of Biomaterials and Biological Interfaces

Redefining the concept of hydration water near soft interfaces

Cite as: Biointerphases **16**, 020801 (2021); https://doi.org/10.1116/6.0000819
Submitted: 25 November 2020 . Accepted: 16 February 2021 . Published Online: 08 March 2021

Fausto Martelli, Carles Calero, and Giancarlo Franzese

Biointerphases
A Journal of Biomaterials and Biological Interfaces

REVIEW

avs.scitation.org/journal/bip

Redefining the concept of hydration water near soft interfaces

Cite as: Biointerphases 16, 020801 (2021); doi: 10.1116/6.0000819
Submitted: 25 November 2020 · Accepted: 16 February 2021 ·
Published Online: 8 March 2021

Fausto Martelli,[1,2,a)] Carles Calero,[3,4,b)] and Giancarlo Franzese[3,4,b)]

AFFILIATIONS

[1]IBM Research Europe, Hartree Centre, Daresbury WA4 4AD, United Kingdom
[2]Department of Physics and CNR Institute of Complex Systems, Sapienza University of Rome, P.le Aldo Moro 2, 00185 Roma, Italy
[3]Secció de Física Estadística i Interdisciplinària, Departament de Física de la Matèria Condensada, Universitat de Barcelona, C. Martí i Franquès 1, 08028 Barcelona, Spain
[4]Institut de Nanociència i Nanotecnologia (IN2UB), Universitat de Barcelona, C. Martí i Franquès 1, 08028 Barcelona, Spain

Note: This paper is part of the Biointerphases Special Topic Collection on Molecular Scale Modeling of Biological Molecules at Interfaces.

[a)]**Electronic mail:** fausto.martelli@ibm.com
[b)]**Electronic addresses:** carles.calero@ub.edu and gfranzese@ub.edu

ABSTRACT

Water determines the properties of biological systems. Therefore, understanding the nature of the mutual interaction between water and biosystems is of primary importance for a proper assessment of any biological activity, e.g., the efficacy of new drugs or vaccines. A convenient way to characterize the interactions between biosystems and water is to analyze their impact on water density and dynamics in the proximity of the interfaces. It is commonly accepted that water bulk density and dynamical properties are recovered at distances of the order of 1 nm away from the surface of biological systems. This notion leads to the definition of *hydration* or *biological* water as the nanoscopic layer of water covering the surface of biosystems and to the expectation that all the effects of the water-interface interaction are limited to this thin region. Here, we review some of our latest contributions, showing that phospholipid membranes affect the water dynamics, structural properties, and hydrogen bond network at a distance that is more than twice as large as the commonly evoked ∼1 nm thick layer and of the order of 2.4 nm. Furthermore, we unveil that at a shorter distance ∼0.5 nm from the membrane, instead, there is an additional interface between lipid-*bound* and *unbound* water. Bound water has a structural role in the stability of the membrane. Our results imply that the concept of hydration water should be revised or extended and pave the way to a deeper understanding of the mutual interactions between water and biological systems.

I. INTRODUCTION

Water is a peculiar substance characterized by a plethora of dynamic and thermodynamic anomalies that make it the only liquid capable of sustaining life as we know it.[1–3] For example, the high heat capacity allows water to absorb and release heat at much slower rates compared to other liquids. As a consequence, water acts as a thermostat that regulates the temperature of our bodies. Overall, seawater shelters our planet from otherwise lethal daily and seasonal temperature variations. Also, water has very low compressibility, which allows blood to be pumped without crystallizing down to the most peripherals and tight vessels delivering oxygen.

Nonetheless, water stabilizes proteins and DNA, restricting access to unfolded states, and shapes the basic structure of cell membranes. Cell membranes are very complex systems made of a large number of components, including proteins, cholesterol, glycolipids, and ionic channels, among others, but their framework is provided by phospholipid molecules forming a bilayer. Being solvated by water, the hydrophilic heads of the phospholipid molecules are exposed to the surrounding solvent molecules, while the hydrophobic tails are arranged side by side, hiding from water and extending in the region between two layers of heads.

Stacked membranes are relevant constituents in several biological structures, including endoplasmic reticulum and Golgi

apparatus, that processes proteins for their use in animal cells, or thylakoid compartments in chloroplasts and cyanobacteria, involved in photosynthesis. When in contact with membranes, water modulates their fluidity and mediates the interaction between different leaflets as well as between membranes and solutes (ions, proteins, DNA, etc.), regulating cell-membrane tasks such as transport and signaling functions.[4] A thin layer of water, with a thickness of only ∼1 nm corresponding to a couple of molecular diameters, hydrates biological systems and is therefore called *biological* or *hydration* water.[5] So far, it has been thought that hydration water is directly responsible for the proper functioning of biological systems,[2] although many issues are still open.[5]

Several experimental techniques have been adopted to study the interaction between hydration water molecules and membrane surfaces. Insights into the orientation of water molecules and on their order have been obtained from vibrational sum frequency generation spectroscopy and nuclear magnetic resonance (NMR) experiments.[6,7] Evidence of enhanced hydrogen bonds (HBs) established between water molecules and the phospholipid heads has been described in experimental investigations from infrared spectroscopy[7,8] and sum frequency generation.[9,10] Nonetheless, far-infrared spectroscopy has shown that resonance mechanisms entangle the motion of phospholipid bilayers with their hydration water.[11] Such complex interactions between water molecules and hydrophobic heads cause perturbations in the dynamical properties of water. NMR spectroscopy has reported a breakdown of the isotropy on the lateral and normal diffusion of water molecules with respect to the surface,[12,13] and rotational dynamics has been the focus of several experimental investigations using ultrafast vibrational spectroscopy,[14] terahertz spectroscopy,[15] and neutron scattering.[16]

Atomistic molecular dynamics (MD) simulations have also been adopted widely to inspect the microscopic details of hydration water (with the obvious drawback of relying on a particular simulation model). The dynamical slow-down of water dynamics due to the interaction with phospholipid membranes reported in NMR experiments[12,13] has been confirmed in MD simulations.[17,18] MD simulations have also provided important insights into the molecular ordering and rotation dynamics in water solvating phospholipid headgroups,[17,19] as well as in quantifying the decay of correlation in water orientational degrees of freedom.[20–24]

Here, we review some of our recent computational investigations on water nanoconfined between stacked phospholipid membranes, reporting evidence that the membrane affects the structural properties of water and its hydrogen bond network (HBN) at distances much larger than the often invoked ∼1 nm. Our results are the outcome of MD simulations of water nanoconfined in phospholipid membranes. Water is described via a modified TIP3P (Ref. 25) model of water. As a typical model membrane, we have used 1,2-dimyristoyl-sn-glycero-3-phosphocholine (DMPC) lipids (Fig. 1). The DMPC is a phospholipid with a hydrophobic tail formed of two myristoyl chains and a hydrophilic head, containing a phosphate and a choline, where the N atom interacts mostly with water oxygen atoms and the P atom interacts mostly with the hydrogen atoms. Choline-based phospholipids are ubiquitous in cell membranes and commonly used in drug-targeting liposomes.[4]

As observed in Ref. 23, at ambient conditions the density profile of water molecules as a function of the distance with respect

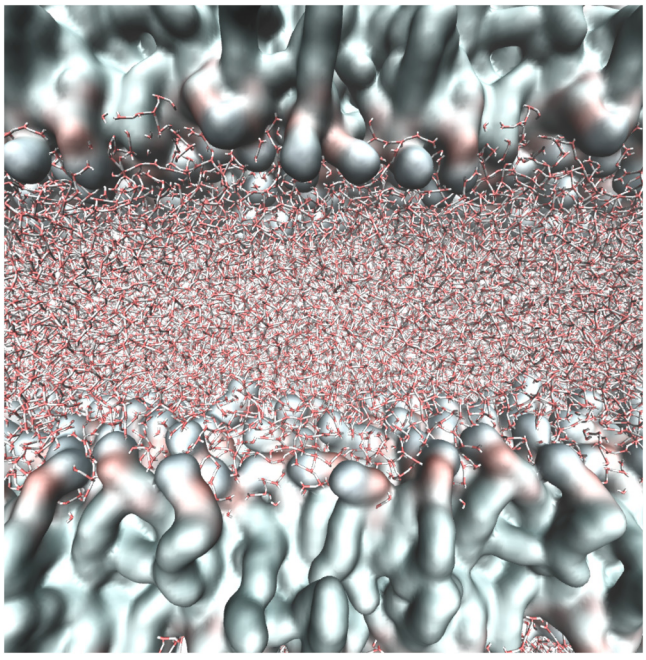

FIG. 1. Representative snapshot of a molecular system composed of water molecules (sticks) and DMPC leaflets (blur fields).

to the average position of the phosphorus atoms in the DMPC lipids displays no layered structure. In fact, due to the thermal fluctuations, it forms a smeared out interface that is ∼1 nm wide, based on the phospholipid head density.[23] However, the interface forms instantaneous layers that can be revealed using several advanced definitions.[26–32] Here, we follow Pandit *et al.*,[26] because it allows us to introduce the instantaneous local distance ξ. The metric ξ is defined as the distance of each water molecule from the closest cell of a Voronoi tessellation centered on the phosphorous and nitrogen atoms of the phospholipid heads (Fig. 2).[22] In the following discussion, ξ should not be confused with the distance δz between water molecules and the average position (over time and space) of the fluctuating lipid surface, calculated along the z-direction orthogonal to the average interface with water. The origin $z = 0$ of this reference system coincides with the center of the lipid bilayer.

II. DYNAMICS

Numerical simulations have shown that hydration water suffers a dramatic slow-down not just in stacked phospholipids,[17,18,20–23,26,33–36] but also in proteins and sugars.[37–41] Insights into the dynamical slow-down can be obtained by inspecting the translational diffusion ($D_{\parallel}$) and rotational dynamics of hydration water molecules. The diffusion coefficient parallel to the surface of the membrane can be obtained from the linear regime reached by the mean squared displacement at

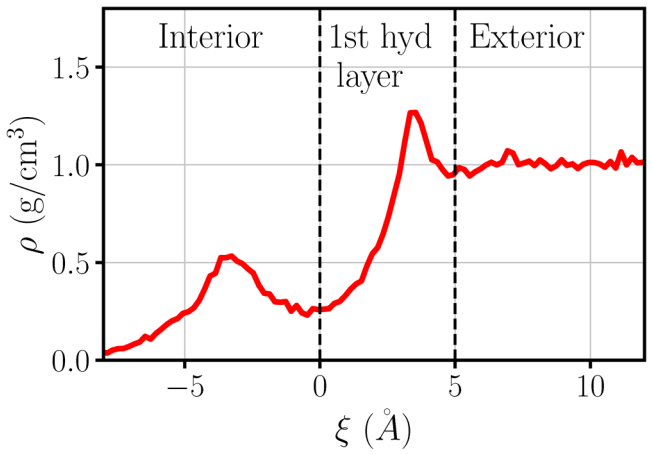

FIG. 2. Density profile ρ of water molecules as a function of the instantaneous local distance ξ from the membrane interface at ambient conditions ($T = 303$ K, average pressure 1 atm, corresponding to bulk density $\rho = 1\,\mathrm{g/cm^3}$) and at the hydration level, defined as the number of water molecules per phospholipid, $\omega = 34$. Water at $\xi < 0$ belongs to the interior of the membrane, while that at $\xi > 5$ Å has the same density as the bulk and can be associated with the exterior of the membrane. The density of water at $0 < \xi < 5$ Å shows a clear maximum revealing the presence of a hydration layer (Ref. 22). At higher density, we observe more than one hydration layer.

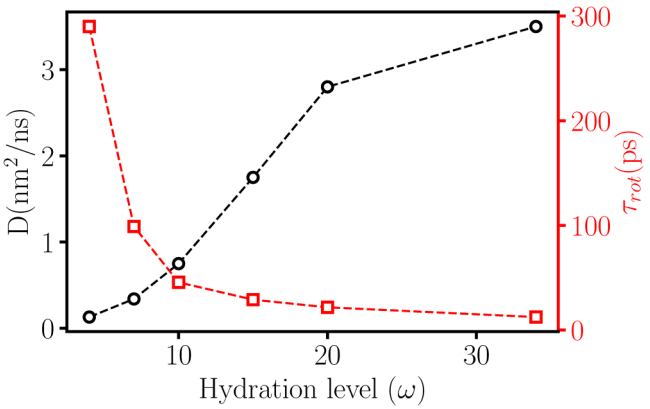

FIG. 3. Dynamics of water molecules between stacked phospholipid bilayers at different hydration level ω at ambient conditions: Diffusion coefficient $D_\parallel$ of water molecules projected on the plane of the membrane (black circles, left vertical axis); rotational relaxation time τ_{rot} of all the water in the system (red squares, right vertical axis). Lines are guides for the eyes.

sufficiently long times from the Einstein relation,

$$D_\parallel \equiv \lim_{t\to\infty} \frac{\left\langle |\mathbf{r}_\parallel(t) - \mathbf{r}_\parallel(0)|^2 \right\rangle}{4t}, \tag{1}$$

where $\mathbf{r}_\parallel(t)$ is the projection of the center of mass of a water molecule on the plane of the membrane and the angular brackets $\langle \cdots \rangle$ indicate average over all water molecules and time origins. Using the DMPC as a model phospholipid membrane, Calero *et al.*[22] have found that water molecules are slowed down by an order of magnitude when the hydration level ω is reduced from 34 to 4 (Fig. 3). This result is in qualitative agreement with experimental and other computational studies.[13–15,20,21] In particular, in conditions of very low hydration, the parallel diffusion is as low as $0.13\,\mathrm{nm^2/ns}$ because water molecules interact with both the upper and the lower leaflets, hence remaining trapped. Increasing the level of hydration ω, Calero *et al.*[22] have shown that $D_\parallel$ increases monotonically. This observation suggests that, increasing the physical separation between the leaflets, the hydration water acts as a screen for the electrostatic interactions between water and the leaflets.

The decreasing interaction of hydration water with the two leaflets can also be observed inspecting the rotational dynamics of water molecules via the rotational dipolar correlation function,

$$C_{\hat{\mu}}(t) \equiv \langle \hat{\mu}(t) \cdot \hat{\mu}(0) \rangle, \tag{2}$$

where $\hat{\mu}(t)$ is the direction of the water dipole vector at time t and $\langle \cdots \rangle$ denotes the ensemble average over all water molecules and time origins. Such a quantity is related to terahertz dielectric relaxation measurements used to probe the reorientation dynamics of water.[15] From Eq. (2), it is possible to define the relaxation time

$$\tau_{rot} \equiv \int_0^\infty C_{\hat{\mu}}(t)dt, \tag{3}$$

which is independent of the analytical form of the correlation function $C_{\hat{\mu}}(t)$. As for $D_\parallel$, the rotational dynamics speeds up with the degree of hydration (Fig. 3), confirming that the interactions between hydration water and the two leaflets modify the overall water dynamics.[14,15,20–22]

To account for the rapidly relaxing signals associated with the reorientation of water molecules in the experiment,[42] Tielrooij *et al.*[15] assumed the existence of three water species near a membrane: (1) bulklike, with characteristic rotational correlation times of a few picoseconds; (2) *fast*, with rotational correlation times of a fraction of picosecond; and (3) irrotational, with characteristic times much larger than 10 ps. Calero *et al.*[22] have shown that it is possible to analyze their simulations using this assumption (Fig. 4); however, the resulting fitting parameters for the correlation times are not showing any regular behavior as a function of ω, questioning the existence of *fast* water near a membrane. This possibility, on the other hand, cannot be ruled out completely, as it could be related to the presence of heterogeneities, such as those associated with water molecules with a single hydrogen bond to a lipid at low hydration.[42]

Nevertheless, Calero *et al.*[22] have shown that a consistent explanation of the changes in the dynamics as a function of ω is reached by observing that, upon increasing the hydration level, water first fills completely the interior of the membrane and next accumulate in layers in the exterior region. The authors rationalized this observation observing that the inner-membrane (or interior) water has an extremely slow dynamics as a consequence of the robustness of water-lipid HBs. Moreover, the water-water HBs

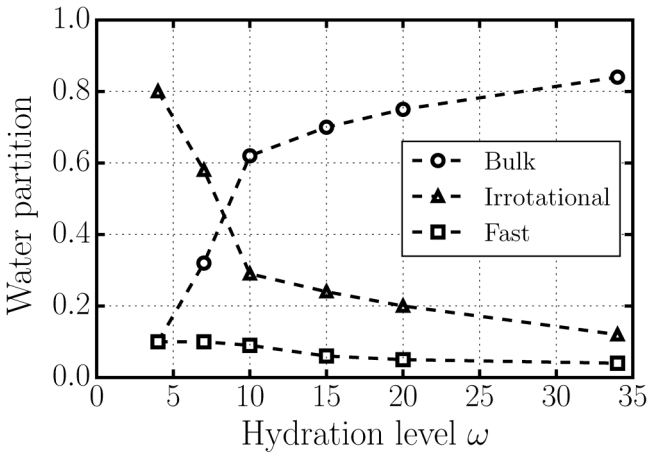

FIG. 4. Partition of membrane hydration water into *fast* (squares), irrotational (triangles), and bulklike (circles) water molecules, following the assumption in Ref. 15, as a function of the hydration level ω. As discussed in Ref. 22, the assumption of the existence of *fast* water leads to inconsistencies.

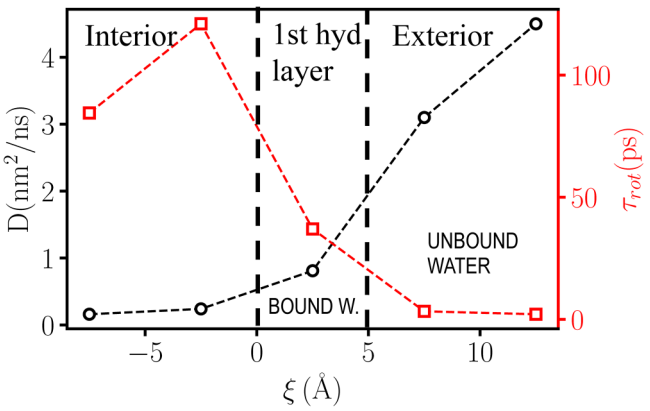

FIG. 5. Dynamics of water molecules between stacked phospholipid bilayers as a function of the instantaneous local distance ξ from the membrane interface at ambient conditions and hydration level $\omega = 34$: Diffusion coefficient $D_{\|}$ of water molecules projected on the plane of the membrane (black circles, left vertical axis); rotational relaxation time τ_{rot} of all the water in the system (red squares, right vertical axis). Lines are guides for the eyes. Vertical dashed lines at $\xi = 0$ and 5 Å mark the interfaces between the water within the interior of the membrane, the first hydration layer of water, and the water exterior to the membrane. The interface at $\xi = 5$ Å separates bound water and unbound water.

within the first hydration layer of the membrane slow down, with respect to bulk water due to the reduction of hydrogen bond switching at low hydration. As shown by Samatas *et al.*,[24] these effects are emphasized when the temperature decreases: water near the membrane has a glassylike behavior when $T = 288.6$ K, with the rotational correlation time of vicinal water, within 3 Å from the membrane, comparable to that of bulk water ≈30 K colder, but with a much smaller stretched exponent, suggesting a larger heterogeneity of relaxation modes.

Both the translational and rotational dynamics of water molecules are strongly determined by their local distance to the membrane. Calero and Franzese[36] have recently shown that the hydration water within the interior of the membrane is almost immobile, the first hydration layer, with $\xi \leq 5$ Å, is *bound* to the membrane, and the exterior water is *unbound* (Fig. 5). The authors have identified the existence of an interface between the bound and the unbound hydration water at which the dynamics undergoes an abrupt change: bound water rotates 63% less than bulk and diffuses 85% less than bulk, while unbound water only 20% and 17%, respectively.

To rationalize the origin of the three dynamically different populations of water, (1) immobile within the membrane interior, (2) bound in the first hydration layer, and (3) unbound at the exterior of the membrane, Calero and Franzese have turned their attention to the investigation of the HBs (Fig. 6). Based on the calculation of the average number of HBs $\langle n_{\mathrm{HB}} \rangle$, they have found that the inner water is an essential component of the membrane that plays a structural role with HBs bridging between lipids, consistent with the previous results.[43,44] In particular, Calero and Franzese have found that, in the case of a fully hydrated membrane, ≈45% of the water-lipids HBs in the interior of the membrane are bridging between two lipids. The fraction of bridging HBs, with respect to the total number of water-lipids HBs, reduces to approximately 1/4 within the first hydration shell. Hence, also the bound

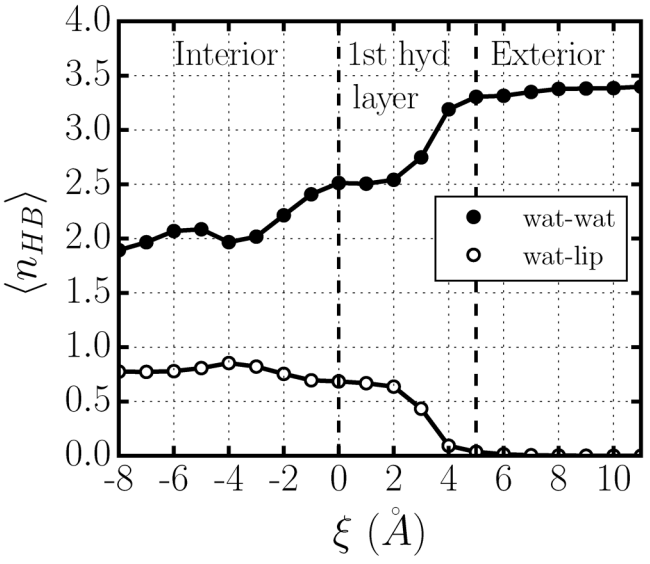

FIG. 6. Average number of HBs $\langle n_{\mathrm{HB}} \rangle$ as a function of the instantaneous local distance ξ from the membrane interface at ambient conditions and hydration level $\omega = 34$. Full circles represent the HBs formed between water molecules, and empty circles the HBs formed by water molecules with selected groups of the phospholipid. Vertical dashed lines at $\xi = 0$ and 5 Å mark the interfaces between the interior, the first hydration layer, and the exterior water of the membrane.

water has a possible structural function for the membrane and, in this sense, can be considered another *constituent* of the membrane that regulates its properties and contributes to its stability. Moreover, they found that unbound hydration water has no water-lipids HBs. However, even at hydration level as low as $\omega = 4$, they find that ≈25% of inner water, and ≈ 18% in the first hydration shell, is unbound, i.e., has only water-water HBs. This could be the possible reason why it has been hypothesized the existence of *fast* water in weakly hydrated phospholipid bilayers in previous works.[15] Nevertheless, as already discussed, Calero and Franzese clearly showed that unbound water is definitely not fast, being at least 1 order of magnitude slower than bulk water.

In order to further rationalize the interactions between hydration water and phospholipid heads, we computed[23] the correlation function

$$C_{\boldsymbol{\delta}}(t) \equiv \langle \boldsymbol{\delta}(t) \cdot \boldsymbol{\delta}(0) \rangle, \tag{4}$$

where $\boldsymbol{\delta}$ is the N-O vector or the P-HO vector. Interestingly, we have found that the P-HO vector has a longer lifetime compared to the N-O vector, indicating that the interactions between P and water hydrogen atoms are stronger than the interactions between N and O.[23] This conclusion is consistent with the observation that the P-HO two-body pair correlation function is characterized by a slightly higher first peak with respect to the N-O first peak two-body pair correlation function (Fig. 7, upper panel).

Starting from the observation that the N-O and the P-HO vectors have different lifetimes, we hypothesized that such a difference can have an effect on the rotational dynamics of hydration water. In particular, we supposed that the rotations around the water dipole moment $\boldsymbol{\mu}$ are different with respect to the rotations around $\overrightarrow{\text{OH}}$ vector. In Ref. 23, we computed $C_{\hat{\mu}}$ and $C_{\overrightarrow{\text{OH}}}$ and we fit the two correlation functions with a double exponential, with characteristic times τ_1 and τ_2, that intuitively reveals the effects of the electrostatic interactions on the slow relaxation. We calculated the relaxation times τ_1 and τ_2 in bins parallel to the membrane surface and centered at increasing distances from the average position of the center of the membrane, z (Fig. 7, middle and lower panels).

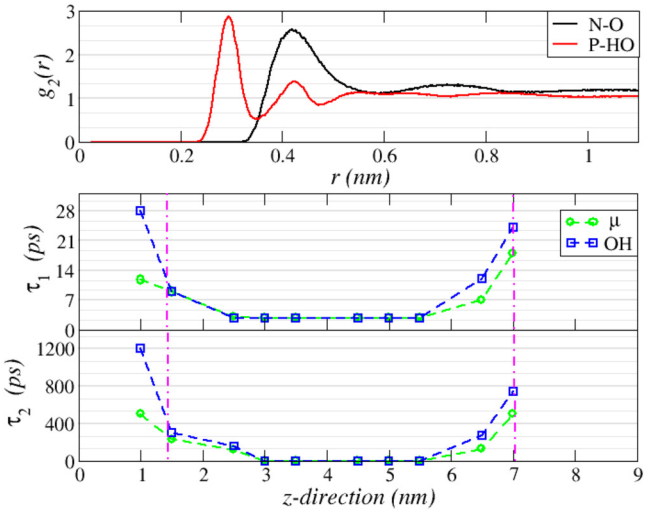

FIG. 7. Upper panel: Two-body pair correlation function computed for the N-O and the P-HO vectors in black and red, respectively, as a function of the relative distance r between the two moieties. Middle and lower panels: *Slow* and *very slow* relaxation times τ_1 and τ_2, respectively, computed for the μ (green open circles) and for the OH (blue open squares) vectors, as a function of the distance z from the center of the lipid bilayer. The magenta lines define the average position of the water-lipid fluctuating surfaces formed by the hydrated bilayer and its image in the system with periodic boundary conditions.

We found that the *slow* relaxation time, τ_1, is orders of magnitude smaller than the *very slow* relaxation time, τ_2. In particular, approaching the membrane, the $\overrightarrow{\text{OH}}$ vector relaxes slower than the $\hat{\mu}$ vector. This is in agreement with the finding that the P-HO interaction is stronger than the N-O interaction. This result can be rationalized by observing that the lipids have different (delocalized) charges on the N-heads and on the P-functional groups and that these charges affect the rotation of water around the two vectors in different ways.

The slowing down of the rotational degrees of freedom (Fig. 7) decreases upon increasing the distance from the membrane surface, δz. In particular, at distances of $\delta z \sim 1.3$ nm from the membrane surface, the relaxation times for the $\hat{\mu}$ vector and for the $\overrightarrow{\text{OH}}$ vector become indistinguishable, as expected in bulk water.

In view of the very high values of the relaxation times in the proximity of the membrane, we hypothesized that the electrostatic interactions with phospholipid heads might cause a slow down in the diffusivity of water molecules comparable—and hence measurable—to that of water at low temperatures.[23] To check our hypothesis, we measured the standard displacement of water molecules in terms of bond units (BUs), defined as the distance traveled by water molecules normalized with respect to the oxygen-oxygen mean distance (which is a temperature-independent quantity), and we compared it with the same quantity of water at supercooled conditions. For a large enough simulated time, a standard displacement of <1 BU would correspond to water molecules rattling in the cage formed by their nearest neighbors. This case would represent a liquid in which the translational degrees of freedom are frozen.

We found that, in the proximity of the membrane surface, water molecules suffer from a dramatic slow-down of ∼60% with respect to the value of bulk water at biological thermodynamic conditions. Moreover, upon increasing the distance from the lipid heads, we found that bulk diffusivity is recovered at ∼1 nm, the domain of definition of hydration water. Considering that the diffusivity of water close to the lipid heads is comparable to that of water at supercooled conditions, we concluded that such a slow-down could be interpreted effectively as a reduction of the thermal energy of water.[23]

III. STRUCTURE

As presented above, the dynamics of bulk water is recovered approximately at ∼1.3 nm away from a membrane surface. However, as we will discuss in the following, the structure analysis of hydration water[23] shows how long-range interactions spread at

much larger distances, opening a completely new scenario for the understanding of water-membrane coupling. In particular, we analyzed[23] how the water intermediate range order (IRO) changes moving away from a membrane.

Modifications in the connectivity of disordered materials induce effects that extend beyond the short range. This is, for example, the case for amorphous silicon and amorphous germanium.[45] Likewise, at specific thermodynamic conditions, water acquires structural properties that go beyond the tetrahedral short range and are comparable to that of amorphous silicon.[46]

In Ref. 23, we adopted a sensitive local order metric (LOM) introduced by Martelli *et al.*[47] to characterize local order in condensed phase. The LOM provides a measure of how much a local neighborhood of a particle j ($j = 1, \ldots, N$) is far from the ground state. For each particle j, the LOM maximizes the spatial overlap between the j local neighborhood, made of M neighbors i with coordinates $\mathbf{P}_i^j$ ($i = 1, \ldots, M$), and a reference structure—the ground state—with coordinates $\mathbf{R}^j$. The LOM is defined as

$$S(j) \equiv \max_{\theta,\phi,\psi;\mathcal{P}} \prod_{i=1}^{M} \exp\left(-\frac{\left|\mathbf{P}_{i_\mathcal{P}}^j - \mathbf{R}^j\right|^2}{2\sigma^2 M}\right), \tag{5}$$

where (θ, ϕ, ψ) are the Euler angles for a given orientation of the reference structure $\mathbf{R}^j$, $i_\mathcal{P}$ are the indices of the neighbors i under the permutation $\mathcal{P}$, and σ is a parameter representing the spread of the Gaussian domain. The parameter σ is chosen such that the tails of the Gaussian functions stretch to half of the O-O distance in the second coordination shell of j in the structure $\mathbf{R}^j$. As reference $\mathbf{R}^j$, we choose the ground state for water at ambient pressure, i.e., cubic ice. The site-average of Eq. (5),

$$S_C \equiv \frac{1}{N}\sum_{j=1}^{N} S(j), \tag{6}$$

is by definition the *score function* and gives a global measure of the symmetry in the system with respect to the reference structure. The LOM and the score function have provided physical insights into a variety of systems,[48–50] hence they are particularly suitable also to characterize[23] and quantify[51] how far the membrane affects the water structural properties.

We found[23] that the overall score function, Eq. (6), for water tends to increase at very short distances from the membrane and is comparable to bulk at $\delta z \gtrsim 1.3$ nm away from the membrane surface (Fig. 8, upper panel). The IRO enhancement is not dramatic but cannot be simply discarded.

Hence, both the dynamics and the IRO are affected as far as ≈1.3 nm away from the membrane surface. Therefore, in Ref. 23, we proposed that the dynamical slow-down and the enhancement of the IRO are two effects related to each other. We suggested that the dynamical slow-down corresponds to an effective reduction of thermal noise that, ultimately, allows water molecules to adjust in slightly more ordered spatial configurations in the proximity of the membrane.

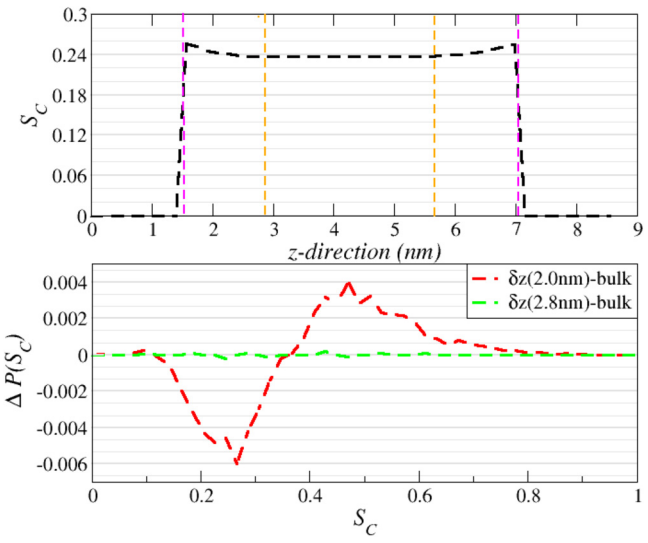

FIG. 8. Score function S_C for water between DMPC membrane leaflets. Upper panel: S_C of water molecules belonging to a bin centered at distance z from the center of the lipid bilayer at 0 and with a bin-width of 1/10 of the entire system. Vertical magenta lines indicate the average positions of the water-lipid interfaces. The majority of water is, on average, in the range between $z = 1.5$ and 7 nm. Vertical dashed orange lines mark the region where S_C approaches the value in bulk water. Lower panel: Water reaches the S_C bulk value only at ≈2.8 nm away from the water-lipid interfaces, as shown by the difference $\Delta P(S_C)$ between the probability density distribution $P(S_C)$ for bulk water and that at a specific distance δz from the average position of the membrane-water interface. Here, we show $\Delta P(S_C)$ for $\delta z = 2.0$ nm (red line), with the bin centered at $z = 3.5$ nm, and for $\delta z = 2.8$ nm (green line), with the bin centered at $z = 4.3$ nm.

Moving away from the membrane, at distances $\delta z \gtrsim 1.3$ nm, S_C seems to reach a plateau, suggesting that a convergence to the bulk value should fall into the distance domain of hydration water. To check this, we computed the probability density distribution $P(S_C)$ of Eq. (6) in the bin centered at $\delta z = 2$ nm away from the surfaces, and we compared it with the distribution of S_C computed in a box of bulk water at the same thermodynamic conditions (Fig. 8, lower panel).

Surprisingly, the two distributions *do not* overlap. This result indicates that the membrane perturbs the structure of water at the intermediate range of, at least, ∼1.6 nm, considering half bin-width. This distance is much larger than that defining hydration water.

We found[51] an overlap between the bulk-water distribution and that for the confined water only if between the two membrane leaflets there is enough water to reach distances as far as $\delta z = 2.8$ nm from the membrane surface. Such a remarkable result indicates that the membrane affects the structural properties of water at least as far as ∼2.4 nm, accounting for the ∼0.4 nm half bin-width. This distance can be considered twice the domain of definition of hydration water.

Therefore, the definition of hydration water, as well as its role, should be extended to account for the repercussion of the membrane on the water structure. Or it should be revised, in order to

further redefine its concept. In order to properly frame our observations into a consistent picture, in addition to our structural analysis of the membrane effects on the water-O positions, we have analyzed next the topology of the HBN that provides another measure of the IRO, but from the perspective of the HBs.

IV. NETWORK TOPOLOGY

The properties of network-forming materials are governed by the underlying network of bonds.[52] However, the topology of this network is very rarely investigated because of the difficulty of such analysis.

A possible approach is through *ring statistics*. It consists of defining, characterizing, and counting the number of closed loops that are made of links (or bonds) between the vertices of the network. Ring statistics allows to study, in particular, the network topology of amorphous systems,[53,54] clathrate hydrates,[55] and chalcogenide glasses.[56] It is, also, an essential tool to characterize continuous random networks.[45,57–61]

After some hesitant debut in the field of water,[62,63] ring statistics has been embraced more and more as a tool to study water properties, starting from its application by Martelli *et al.* to characterize the transformations in the bulk-water HBN near the liquid-liquid critical point.[64] Since then, ring statistics has been an essential tool for investigating the properties of water in its liquid phase,[52,65–67] as well as its amorphous states,[47,48,52] and for inspecting the dynamics of homogeneous nucleation.[68–70]

Based on the idea that the connectivity in network-forming materials governs their properties, we explored how the topology of the HBN changes when water is confined between phospholipid membranes.[51] In fact, the HBN is what differentiates water from "simple" liquids.[71]

In water, the HBN is directional. Hence, there are several ways for defining and counting rings. Formanek and Martelli showed that each of these possibilities carries different but complementary, physical meaning.[52]

Here, we use a definition for the HB that was initially introduced by Luzar and Chandler[72] and is common in the field. However, other definitions are possible, due to our limited understanding of the HBs. Nevertheless, it has been shown that all these definitions have a satisfactory qualitative agreement over a wide range of thermodynamic conditions.[73,74]

In Fig. 9, we present three possible ways of defining rings in a directional network, as in the case of water. The first (Fig. 9, top) explicitly looks for the shortest ring[75] starting from molecule 1, when this molecule donates one HB, regardless of whether other molecules in the ring accept or donate a bond. This definition emphasizes the intrinsic directional nature of the HBN. The second definition (Fig. 9, center) considers only the shortest ring formed when molecule 1 can only accept an HB. The third definition (Fig. 9, bottom), adopted by Formanek and Martelli,[52] ignores both the donor/acceptor nature of the starting molecule and the shortest rings restriction, leading to a higher number of rings. The reader can refer to the original work[52] for further details about the definitions and their physical meaning in the case of bulk liquid and glassy water at several thermodynamic conditions.

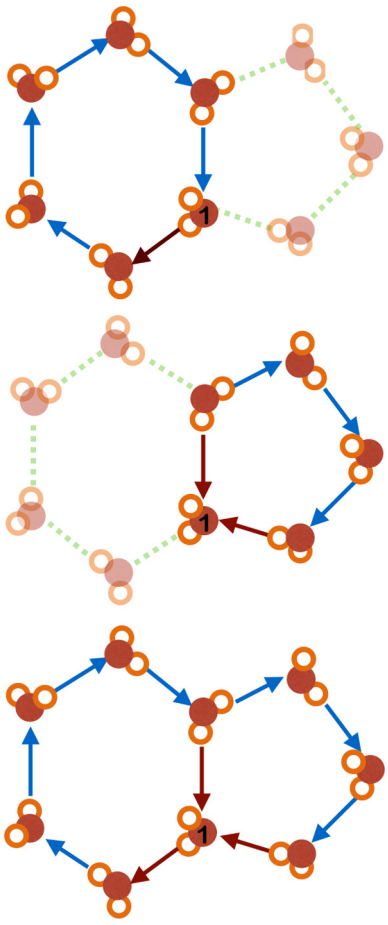

FIG. 9. Schematic representation of three possible ways of defining the rings in the water directional network. In each case, we start counting from the water molecules labeled as 1, with O atoms in solid brown and H atoms in white, and we follow the directional HBs from H to O (arrows) along the HBN, until we return to molecule 1 or until we exceed 12 steps. We consider only rings that cannot be decomposed into subrings. Top: A ring is formed only when molecule 1 donates HBs (brown arrow). In the example, the shortest ring is the hexagonal one (blue arrows). Center: A ring is formed when molecule 1 donates or accepts (brown arrows) HBs. In the example, the shortest ring is the pentagonal ring (arrows). Bottom: Any ring formed by molecule 1 is considered, starting from any of its HBs (brown arrows), without bond or ring's length constraints. In the example, there are a hexagonal and a pentagonal ring. Martelli *et al.* adopted the latter definition in Ref. 51.

The authors of Ref. 51 computed the probability of having a n-folded ring, $P(n)$, as a function of the distance δz from the membrane. They found that near the membrane the $P(n)$ is strikingly different from that of bulk water (Fig. 10, upper panel). In particular, the distribution is richer in hexagonal and shorter rings and is poorer in longer rings.

This result points toward two main conclusions: (1) For membrane-hydration water, at a distance $\delta z \leq 0.8$ nm, the HBN tends to be preferentially icelike, i.e., dominated by hexagonal

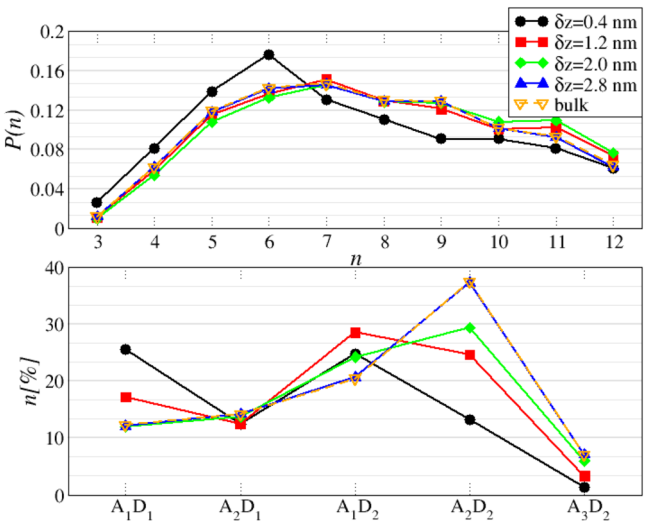

FIG. 10. HBN ring statistics at a distance δz from the average position of the fluctuating membrane and in bulk water. In both panels, the sets of data are for bulk water (open orange triangles), and $\delta z = 0.4$ nm (black dots), 1.2 nm (red squares), 2.0 nm (green diamonds), and 2.8 nm (blue triangles). Quantities at a given distance δz from the membrane surface are calculated in 0.8 nm-wide bins centered at δz. Upper panel: Probability of having n-member rings, $P(n)$. All $P(n)$ are normalized to unity and, therefore, do not reflect the total number of rings of a given size. Lower panel: Percentage-wise decomposition of the HBs per water molecule into acceptor (A) and donor (D). The x-axis labels A_xD_y indicate the number of acceptor (A_x) and donor (D_y) HBs, respectively, of the configurations schematically represented in the plot (with the oxygen of central water molecule in blue). For clarity, we omit combinations with minor contributions, e.g., A_3D_1, A_0D_y, and A_xD_0.

rings. This observation is consistent with the results, discussed in Secs. I–III, showing that membrane-vicinal water is characterized by enhanced IRO and slower dynamics than bulk water. (2) The reduced number of longer rings in the hydration water is consistent with the reduction of the overall dimensionality of the system due to the interface. The membrane fluctuating surface reduces the available space for the HBN in the first layer of hydration water.

All the $P(n)$ calculated at larger distances, $\delta z > 0.8$ nm, are quite different from that of the hydration water and gradually converge toward the bulk case upon increasing δz. In particular, the probability of hexagonal rings decreases progressively, while longer rings become more and more frequent.

This sudden change in $P(n)$, between the first and the following bins, is consistent with the results, discussed in Secs. I–III, demonstrating the existence of a drastic change in structure and dynamics between bound water, in the first hydration layer, and unbound water, away from the membrane.[36] Here, the border between the two regions is increased from ∼0.5 (Ref. 36) to ∼0.8 nm due to the membrane fluctuations, that are not filtered out in Ref. 51, and to the spatial resolution, i.e., the bin size, of the analysis.

The HBN of bulk water is finally recovered in the bin centered at $\delta z = 2.8$ nm away from the membrane surface, i.e., for $\delta z \geq 2.4$ nm. Remarkably, this distance corresponds to the same at which water recovers the IRO of bulk water,[23] as discussed in the Sec. II. This important result indicates a clear connection between the structural properties of water molecules and the topology of the HBN, while further pointing toward the necessity of revising the concept of hydration water.

The quality of the HBN, in terms of broken and intact HBs, is a tool of fundamental importance to fully cast the topology of the HBN in a consistent and complete physical framework. As a matter of fact, the presence of coordination defects affects the fluidity of water and is directly related to its capability of absorbing long-range density fluctuations.[46] Therefore, the authors in Ref. 51 complemented their investigation of the HBN topology with the analysis of its quality.

They decomposed the HBs per water molecule into acceptor-(A) and donor-(D) types (Fig. 10, lower panel). They label as A_2D_2 a water molecule with perfect coordination, i.e., donating two bonds and accepting two bonds and as A_xD_y the others accepting x and donating y bonds. They focused their attention on the following coordination configurations: A_1D_1, A_2D_1, A_1D_2, A_2D_2, and A_3D_2, as other configurations do not contribute significantly. First, they checked that in bulk water, at ambient conditions, the predominant configuration is A_2D_2. For the TIP3P model of water, this configuration accounts for ∼35% of the total composition. The second most dominant configuration in bulk is A_1D_2 with ∼20%, followed by A_2D_1 with ∼13%, A_1D_1 with ∼12% and, finally, A_3D_2 accounting for less than 10% (Fig. 10, lower panel).

Such distribution qualitatively reflects the distribution in *ab initio* liquid water at the same thermodynamic conditions.[76] Hence, it suggests that classical potentials can carry proper physical information even in very complex systems such as biological interfaces.

In the proximity of the membrane, the network of HBs largely deviates from that of bulk water, except for the under-coordinated configuration A_2D_1. In particular, the coordination defects A_1D_1 and A_1D_2 dominate the distribution, with ∼25% each, followed by the configurations A_2D_1 and A_2D_2, with ∼15% each, and a minor percentage of higher coordination defects A_3D_2, with ∼3%.

However, the small percentage of perfectly coordinated configurations, A_2D_2, near the membrane seems inconsistent with the higher local order observed at the same distance,[23,51] and with the enhanced hexagonal ring statistics of the HBN,[51] already discussed. Such discrepancy is only apparent for the following two reasons.

First, both the structural score function, S_C, and the ring statistics are a measure of the IRO beyond the short range. On the contrary, the quality of the HBN, in terms of defects, is a measure only of the short-range order.

Second, the defects analysis includes only HBs between water molecules and does not account for the strong HBs between water molecules and the phospholipid headgroups. Instead, as discussed in Sec. II,[36] ∼30% of the water molecules in the first hydration shell are bound to the membrane with at least one HB.

Away from the membrane, upon increasing the distance, Martelli *et al.*[51] observed a progressive enhancement of perfectly tetra-coordinated configurations (Fig. 10, lower panel). They found a progressive depletion of all coordination defects, up to recovering

the bulk-water case at a distance of $\delta z \geq 2.4$ nm from the membrane surface, as for the probability distribution of S_C and the HBN topology.

The intriguing evidence that the under-coordinated defect A_2D_1 remains almost constant at all distances is, for the moment, not explained. Indeed, it could be due to a variety of reasons, going from the presence of water-membrane HBs in the first hydration layer to the propagation of defects in bulk, and it would require a detailed study.

V. CONCLUSIONS AND FUTURE RESEARCH DIRECTIONS

The results summarized in this short review question our common understanding of hydration water near soft membranes, such as those in biological systems. This water layer, often called biowater, is usually considered ∼1 nm wide and is regarded as the amount of water that directly shape and define the biological activity in proteins, cells, DNA, etc. Such definition has been proposed based on results, both from experiments and computations, showing that the water dynamics and density are affected by the biological interface within ∼1 nm while they recover the bulk behavior at larger distances.

In our calculations based on well-established models of water nanoconfined between DMPC membranes, instead, we found new evidence that indicates the need for a revised definition of hydration water. Our findings should be taken into account (1) when interpreting experimental results, (2) when developing membrane-water effective interaction potentials, and (3) when exploring the role of hydration water in biological processes at large. We achieved this conclusion by focusing on physical quantities that have been not thoroughly, or not at all, considered before.

In particular, by considering the instantaneous local distance of water from the membrane, Calero and Franzese were able to unveil the existence of a new interface between bound and unbound water ∼0.5 nm away from the membrane-water interface.[36] Bound water behaves like a structural component of the membrane and has translational and rotational dynamics that are intermediate between the water inside and outside the membrane.[36] Bound-water dynamics is dominated by the strong HB with the membrane and is orders of magnitude slower than the unbound water. We recover the dynamics of bulk water only ∼1.3 nm away from the membrane.

However, we showed that the membrane interface has an effect on the structure of the hydration water at a distance almost twice as large, up to, at least, ∼2.4 nm.[23] We got such a result by analyzing how the water structure and IRO change by moving away from the membrane. To this goal, we evaluated the score function, a structural observable that quantifies how close is the local structure to a reference configuration: in our case, the cubic ice. Again, we found that water ∼1.3 nm away from the membrane has a small but measurable IRO enhancement.

Hence, both the dynamics and the structure of hydration water undergo an effective reduction of the thermal noise within the ∼1.3 nm thick layer near the membrane. We interpret it as a consequence of the interaction of water with the membrane. Also, we showed that different chemical species constituting the lipid heads interact with water molecules with different strengths, hence providing a rationale for the contributions to the observed dynamical slow-down in the proximity of the surface.[23]

Furthermore, Martelli *et al.*[51] analyzed the IRO from the HB perspective by studying the HBN topology and its ring statistics. They found that water within ∼0.8 nm from the average position of the fluctuating membrane has an excess of hexagonal and shorter rings and a lack of longer rings with respect to bulk water.

Moreover, the defect analysis of the HBN showed that water in this ∼0.8 nm-wide layer has a lack of water-tetra-coordinated molecules and an excess of water bi-coordinated molecules. This result does not contradict the enhanced water IRO within the same layer because the HBN-defects analysis measures only the short-range order and does not account for the water-membrane HBs.

Also, Martelli *et al.*[51] found a sudden change in the HBN around 0.8 nm, with a ring statistics that approaches that of bulk. This result confirms the qualitative difference between bound and unbound water.[36]

The analysis of the HBN ring statistics and the HBN defects shows that the membrane interface generates perturbations in the ring statistics that extends as far as, at least, ∼2.4 nm.[51] This observation corroborates that the soft interface affects water structure up to a distance at least twice as long as that usually associated with the hydration water.

Our conclusions entail further investigation about the relationship between diseases, possibly promoted by extracellular matrix variations, e.g., of hydration or ionic concentration, with the water HBN rearrangements. Examples of such illnesses are cardiac disease and arterial hardening, such as the effect of hypohydration on endothelial function as discussed in Ref. 77 or the atherosclerosis and the inflammatory signaling in endothelial cells as explained in Ref. 78. Readers interested in learning about the many examples of how hydration plays a role in the development of various morbidities—going from chronic renal failure to glaucoma—are encouraged to read specialized reviews, such as Ref. 79, and the references therein. Here, we limit ourselves to observe that variations of ionic concentration drastically change the water HBN structure[80] and dynamics,[81] affecting the solubility of transmembrane proteins and possibly inducing dysfunction in receptor binding[82] or membrane channels.[83] Furthermore, while salt-concentration variations have an effect on hydration water that is similar to an increase in pressure,[84] dehydration affects the water structure and dynamics near the membrane in a way similar to a decrease in temperature.[36]

In particular, we foresee the extension of these calculations to out-of-equilibrium cases. Indeed, it has been recently shown that the potency of antimicrobial peptides may not be a purely intrinsic chemical property and, instead, depends on the mechanical state of the target membrane,[85] which varies at normal physiological conditions.

ACKNOWLEDGMENTS

F.M. acknowledges support from the STFC Hartree Centre's Innovation Return on Research programme, funded by the Department for Business, Energy and Industrial Strategy. C.C. and G.F. acknowledge the support of Spanish grant (No. PGC2018-099277-B-C22) (MCIU/AEI/ERDF), and G.F.

acknowledges the support by the ICREA Foundation (ICREA Academia prize).

DATA AVAILABILITY

The data that support the findings of this study are available from the corresponding author upon reasonable request.

REFERENCES

[1]*Water and Life*, edited by R. Lynden-Bell, S. Morris, J. Barrow, J. Finney, and C. Harper (CRC, Boca Raton, 2010).
[2]M. Chaplin, Nat. Rev. Mol. Cell. Biol. **7**, 861 (2006).
[3]P. Ball, ChemPhysChem **9**, 2677 (2008).
[4]W. Hamley, *Introduction to Soft Matter* (John Wiley and Sons, West Sussex, 2007).
[5]D. Zhong, S. K. Pal, and A. H. Zewail, Chem. Phys. Lett. **503**, 1 (2011).
[6]S. König, E. Sackmann, D. Richter, R. Zorn, C. Carlile, and T. Bayerl, J. Chem. Phys. **100**, 3307 (1994).
[7]X. Chen, W. Hua, Z. Huang, and H. C. Allen, J. Am. Chem. Soc. **132**, 11336 (2010).
[8]H. Binder, Appl. Spectrosc. Rev. **30**, 15 (2003).
[9]T. Ohto, E. H. G. Backus, C.-S. Hsieh, M. Sulpizi, M. Bonn, and Y. Nagata, J. Phys. Chem. Lett. **6**, 4499 (2015).
[10]M. Deiseroth, M. Bonn, and E. H. G. Backus, Phys. Chem. Chem. Phys. **22**, 10142 (2020).
[11]G. DÁngelo, V. Conti Nibali, C. Crupi, S. Rifici, U. Wanderlingh, A. Paciaroni, F. Sacchetti, and C. Branca, J. Phys. Chem. B **121**, 1204 (2017).
[12]F. Volke, S. Eisenblätter, S. Galle, and G. Klose, Chem. Phys. Lipids **70**, 121–131 (1994).
[13]S. R. Wassall, Biophys. J. **71**, 2724 (1996).
[14]W. Zhao, D. E. Moilanen, E. E. Fenn, and M. D. Fayer, J. Am. Chem. Soc. **130**, 13927 (2008).
[15]K. J. Tielrooij, D. Paparo, L. Piatkowski, H. J. Bakker, and M. Bonn, Biophys. J. **97**, 2848 (2009).
[16]M. Trapp, T. Gutberlet, F. Juranyi, T. Unruh, B. Demé, M. Tehei, and J. Peters, J. Chem. Phys. **133**, 164505 (2010).
[17]M. L. Berkowitz, D. L. Bostick, and S. Pandit, Chem. Rev. **106**, 1527 (2006).
[18]S. Y. Bhide and M. L. Berkowitz, J. Chem. Phys. **123**, 224702 (2005).
[19]R. W. Pastor, Curr. Opin. Struct. Biol. **4**, 486 (1994).
[20]Z. Zhang and M. L. Berkowitz, J. Phys. Chem. B **113**, 7676 (2009).
[21]S. M. Gruenbaum and J. L. Skinner, J. Chem. Phys. **135**, 075101 (2011).
[22]C. Calero, H. E. Stanley, and G. Franzese, Materials **9**, 319 (2016).
[23]F. Martelli, H.-Y. Ko, C. C. Borallo, and G. Franzese, Front. Phys. **13**, 136801 (2018).
[24]S. Samatas, C. Calero, F. Martelli, and G. Franzese, *Water Between Membranes: Structure and Dynamics*, Number 4 in Series in Computational Biophysics, 1st ed. (CRC, New York, 2019), p. 69, ISBN 9781498799799.
[25]W. L. Jorgensen, J. Chandrasekhar, and J. D. Madura, J. Chem. Phys. **79**, 926 (1983).
[26]S. A. Pandit, D. Bostick, and M. L. Berkowitz, J. Chem. Phys. **119**, 2199 (2003).
[27]D. T. Allen, Y. Saaka, L. C. Pardo, M. J. Lawrence, and C. D. Lorenz, Phys. Chem. Chem. Phys. **18**, 30394 (2016).
[28]E. Chacón and P. Tarazona, Phys. Rev. Lett. **91**, 166103 (2003).
[29]H. Martínez, E. Chacón, P. Tarazona, and F. Bresme, Proc. R. Soc. London, Ser. A **467**, 1939 (2011).
[30]A. P. Willard and D. Chandler, J. Phys. Chem. B **114**, 1954 (2010).
[31]M. Sega, S. S. Kantorovich, P. Jedlovszky, and M. Jorge, J. Chem. Phys. **138**, 044110 (2013).
[32]R. M. Ziolek, F. Fraternali, A. Dhinojwala, M. Tsige, and C. D. Lorenz, Langmuir **36**, 447 (2020).
[33]T. Róg, K. Murzyn, and M. Pasenkiewicz-Gierula, Chem. Phys. Lett. **352**, 323 (2002).
[34]F. C. Lopez, S. O. Nielsen, M. L. Klein, and P. B. Moore, J. Phys. Chem. B **108**, 6603 (2004).
[35]J. Yang, C. Calero, and J. Martí, J. Chem. Phys. **140**, 104901 (2014).
[36]C. Calero and G. Franzese, J. Mol. Liq. **273**, 488 (2019).
[37]G. Camisasca, A. Iorio, M. De Marzio, and P. Gallo, J. Mol. Liq. **268**, 903 (2018).
[38]A. Iorio, G. Camisasca, M. Rovere, and P. Gallo, J. Chem. Phys. **51**, 044507 (2019).
[39]A. Iorio, G. Camisasca, and P. Gallo, Sci. China Phys. Mech. **62**, 107011 (2019).
[40]A. Iorio, G. Camisasca, and P. Gallo, J. Mol. Liq. **282**, 617 (2019).
[41]A. Iorio, M. Minozzi, G. Camisasca, M. Rovere, and P. Gallo, Philos. Mag. **100**, 1 (2020).
[42]V. V. Volkov, D. J. Palmer, and R. Righini, Phys. Rev. Lett. **99**, 078302 (2007).
[43]M. Pasenkiewicz-Gierula, Y. Takaoka, H. Miyagawa, K. Kitamura, and A. Kusumi, J. Phys. Chem. A **101**, 3677 (1997).
[44]C. F. Lopez, S. O. Nielsen, M. L. Klein, and P. B. Moore, J. Phys. Chem. B **108**, 6603 (2004).
[45]F. Wooten, K. Winer, and D. Weaire, Phys. Rev. Lett. **54**, 1392 (1985).
[46]F. Martelli, S. Torquato, N. Giovambattista, and R. Car, Phys. Rev. Lett. **119**, 136002 (2017).
[47]F. Martelli, H.-Y. Ko, E. C. Oğuz, and R. Car, Phys. Rev. B **97**, 064105 (2016).
[48]F. Martelli, N. Giovambattista, S. Torquato, and R. Car, Phys. Rev. Mater. **2**, 075601 (2018).
[49]F. Martelli, J. Chem. Phys. **150**, 094506 (2019).
[50]B. Santra, H.-Y. Ko, Y.-W. Yeh, F. Martelli, I. Kaganovich, Y. Raitses, and R. Car, Nanoscale **10**, 22223 (2018).
[51]F. Martelli, J. Crain, and G. Franzese, ACS Nano **14**, 8616 (2020).
[52]M. Formanek and F. Martelli, AIP Adv. **10**, 055205 (2020).
[53]S. Le Roux and P. Jund, Comput. Mater. Sci. **49**, 70 (2010).
[54]X. Yuan and A. N. Cormack, Comput. Mater. Sci. **24**, 343 (2002).
[55]V. Chihaia, S. Adams, and W. F. Kuhs, Chem. Phys. **317**, 208 (2005).
[56]S. Blaineau and P. Jund, Phys. Rev. B **69**, 064201 (2004).
[57]F. Wooten, Acta Crystallogr. A **58**, 346 (2002).
[58]B. R. Djordjevic, M. F. Thorpe, and F. Wooten, Phys. Rev. B **52**, 5685 (1985).
[59]G. T. Barkema and N. Mousseau, Phys. Rev. Lett. **71**, 4358 (1996).
[60]G. T. Barkema and N. Mousseau, Phys. Rev. B **62**, 4985 (2000).
[61]T. S. Hudson and P. Harrowell, J. Chem. Phys. **126**, 184502 (2007).
[62]R. Martoňák, D. Donadio, and M. Parrinello, Phys. Rev. Lett. **92**, 225702 (2004).
[63]R. Martoňák, D. Donadio, and M. Parrinello, J. Chem. Phys. **122**, 134501 (2005).
[64]J. C. Palmer, F. Martelli, Y. Liu, R. Car, A. Z. Panagiotopoulos, and P. G. Debenedetti, Nature **510**, 385 (2014).
[65]B. Santra, R. A. DiStasio Jr., F. Martelli, and R. Car, Mol. Phys. **113**, 2829 (2015).
[66]G. Camisasca, D. Schlesinger, I. Zhovtobriukh, G. Pitsevich, and L. G. M. Pettersson, J. Chem. Phys. **151**, 034508 (2019).
[67]F. Martelli, e-print arXiv:2101.09160[cond-mat.soft], 2021.
[68]J. Russo and H. Tanaka, Nat. Commun. **5**, 3556 (2014).
[69]F. Leoni, R. Shi, H. Tanaka, and J. Russo, J. Chem. Phys. **151**, 044505 (2019).
[70]M. Fitzner, G. C. Sosso, S. J. Cox, and A. Michaelides, Proc. Natl. Acad. Sci. U.S.A. **116**, 2009 (2019).
[71]L. Pauling, *The Nature of the Chemical Bond, and the Structure of Molecules and Crystals*, 3rd ed. (Cornell University, Ithaca, NY, 1960).
[72]A. Luzar and D. Chandler, Nature **379**, 55 (1996).
[73]D. Prada-Gracia, R. Shevchuk, and F. Rao, J. Chem. Phys. **139**, 084501 (2013).
[74]R. Shi, J. Russo, and H. Tanaka, J. Chem. Phys. **149**, 224502 (2018).
[75]S. V. King, Nature **213**, 1112 (1967).
[76]R. A. DiStasio Jr., B. Santra, Z. Li, X. Wu, and R. Car, J. Chem. Phys. **141**, 084502 (2014).
[77]G. Arnaoutis, S. A. Kavouras, N. Stratakis, M. Likka, A. Mitrakou, C. Papamichael, L. S. Sidossis, and K. Stamatelopoulos, Eur. J. Nutr. **56**, 1211 (2017).

[78]N. I. Dmitrieva and B. B. Maurice, PLoS ONE **10**, 1 (2015).
[79]F. Manz, J. Am. Coll. Nutr. **26**, 535S (2007).
[80]R. Mancinelli, A. Botti, F. Bruni, M. A. Ricci, and A. K. Soper, Phys. Chem. Chem. Phys. **9**, 2959 (2007).
[81]M. D. Fayer, D. E. Moilanen, D. Wong, D. E. Rosenfeld, E. E. Fenn, and S. Park, Acc. Chem. Res. **42**, 1210 (2009).
[82]M. Li and J. Song, Biochem. Biophys. Res. Commun. **360**, 128 (2007).
[83]D. Ma, T. S. Tillman, P. Tang, E. Meirovitch, R. Eckenhoff, A. Carnini, and Y. Xu, Proc. Natl. Acad. Sci. **105**, 16537 (2008).
[84]P. Gallo, D. Corradini, and M. Rovere, J. Mol. Liq. **189**, 52 (2014).
[85]V. Losasso, Y.-W. Hsiao, F. Martelli, M. Winn, and J. Crain, Phys. Rev. Lett. **122**, 208103 (2019).